Phonon conductivity of doped germanium under uniaxial stress in the [110] direction

K. C. Sood and M. K. Roy*
Department of Physics, Banaras Hindu University, Varanasi 221005, India
(Received 9 April 1992; revised manuscript received 11 June 1992)

The relaxation-rate expressions for elastic, inelastic, and absorption phonon-electron processes in n-type germanium have been derived under [110] directional uniaxial tension. Using these expressions, the phonon conductivity of Sb-doped Ge under tension is evaluated and compared with the experimental results given by Keyes and Sladek. It is found that a slight increase of Bohr radii of the upper two levels of the donor ground states and decrease of shear deformation potential E_u with stress can give better agreement with the experimental results. This work suggests that the theory of electron-phonon interaction is not a failure, as suspected by earlier workers.

I. INTRODUCTION

Although Keyes and Sladek[1] measured the phonon conductivity κ of Sb-doped Ge in 1962, the qualitative features of the experimental results have not been explained satisfactorily. The regular decrease of the thermal resistivity with stress at a constant temperature in the liquid-He-temperature region is the main source of trouble. Theoretically,[2,3] a peak was qualitatively expected at a particular stress and later on Suzuki[4] after quantitative treatment of the problem in the [111] direction arrived at the same result. Suzuki[5] also applied his theory on ultrasonic attenuation in Sb-doped Ge with no success, which forced him to assume the presence of internal stress in the sample. Other workers[6,7] have also used the idea of the presence of internal stress to explain the phonon conductivity of Sb-doped Ge at low temperatures but their calculations are more or less parametric in approach and the ground-state wave functions have been taken to be independent of the internal stress. Since the phonon scattering by bound electrons is very sensitive to the detailed nature of the donor ground state, the knowledge of electron-phonon interaction via related properties can also give information about the donor state under stress. Realizing this, we derive here the expressions of $\tau_{e\text{-ph}}^{-1}$ in the presence of uniaxial stress in the [110] direction using the anisotropic form factor. A theoretical analysis of the phonon conductivity of Sb-doped Ge under uniaxial stress is then given. The possible reason for a discrepancy between the theory and experiment in the [111] direction is also pointed out.

II. THEORY

A. The donor ground state under uniaxial stress

The ground state of the donor electron in a many-valley semiconductor, in the effective-mass approximation, is

$$\psi_n(\bar{r})=\sum_j \alpha_j^n F_j(\bar{r})\phi_j(\bar{r}) \ . \tag{1}$$

In Ge, there are four valleys and j runs from 1 to 4. $F_j(\bar{r})$ is the hydrogenlike envelope function and $\phi_j(\bar{r})$ are the Bloch states. Valley-orbit interaction splits the four-fold degenerate state into a singlet and a triplet state. Kohn and Luttinger[8] calculated the values of α_j^n for such a system. In the presence of stress, $\psi(\bar{r})$ should be perturbed and the degeneracy of the triplet state, in general, should also be lifted. Many workers[9-11] have solved the problem theoretically with the approximation that $F_j(\bar{r})$ and $\phi_j(\bar{r})$ remain unaffected under low uniaxial stress. Only α_j's are assumed to be perturbed. We report here the calculations of α_j's due to Gorman and Solin[11] when the uniaxial stress is in the [110] direction:

$$\begin{aligned} &\alpha_j^0: \ \alpha_1 \quad \beta_1 \quad \alpha_1 \quad \beta_1; \quad \alpha_j^1: \ \frac{1}{\sqrt{2}} \quad 0 \quad -\frac{1}{\sqrt{2}} \quad 0; \\ &\alpha_j^2: \ 0 \quad -\frac{1}{\sqrt{2}} \quad 0 \quad \frac{1}{\sqrt{2}}; \quad \alpha_j^3: \ \beta_1 \quad -\alpha_1 \quad \beta_1 \quad -\alpha_1, \end{aligned} \tag{2}$$

where

$$\alpha_1=\tfrac{1}{2}(1+\gamma_b)^{1/2}, \quad \beta_1=\tfrac{1}{2}(1-\gamma_b)^{1/2} ,$$

and

$$\gamma_b=\frac{\varepsilon_b}{(4+\varepsilon_b^2)^{1/2}}, \quad \varepsilon_b=\frac{E_u S_{44} X}{4\Delta} \ .$$

E_u is the shear deformation potential, 4Δ is the chemical shift in the absence of stress (see Table I), S_{44} is the elastic shear constant, and X is the tension. The form of $F_j(\bar{r})$ is available in Ref. 9. The energy corresponding to different $\psi_n(\bar{r})$ under [110] stress is

$$\varepsilon_0=\Delta[-1-2(1+\tfrac{1}{9}\varepsilon_b^2)^{1/2}],\quad \varepsilon_1=\Delta(1-\tfrac{2}{3}\varepsilon_b)\ ,$$
$$\varepsilon_2=\Delta(1+\tfrac{2}{3}\varepsilon_b),\quad \varepsilon_3=\Delta[-1+2(1+\tfrac{1}{9}\varepsilon_b^2)^{1/2}]\ . \tag{3}$$

We observe that a singlet-triplet system becomes a nondegenerate four-level system under the influence of uniaxial stress in the [110] direction. Figure 1 shows the energy levels with varying (tensile) stress.

B. Phonon-electron relaxation rates $\tau_{e\text{-ph}}^{-1}$

The thermal equilibrium populations, required for the calculations of $\tau_{e\text{-ph}}^{-1}$, of these levels, are obtained to be

$$f_0(T)=\left[1+\sum_{l=1}^{3}e^{-\Delta_{l0}/k_BT}\right]^{-1},\qquad f_l(T)=f_0(T)e^{-\Delta_{l0}/k_BT}, \tag{4}$$

with $l=1,2,3$ and $\Delta_{mn}=\varepsilon_m-\varepsilon_n$. Now starting from the electron-phonon matrix element[12] in between the mth and nth levels, we can calculate the relaxation rates for the elastic, inelastic, and thermally assisted phonon absorption processes. Suzuki[5] did not derive the expressions for $\tau_{e\text{-ph}}^{-1}$ (inel), inelastic, and $\tau_{e\text{-ph}}^{-1}$(ab), thermally assisted phonon absorption processes.

1. *Elastic processes*

The energy conservation for the elastic process is as follows:

$$1s(n)+\hbar\omega_{q\lambda}\rightleftharpoons\text{Int.}\ ,\quad 1s(m)\rightleftharpoons 1s(n')+\hbar\omega_{q'\lambda'}\ ,$$

where Int. denotes appropriate intermediate states. Here m can take on any values 0 to 3 for any given initial state n. For completeness we have derived the relaxation rates in the second-order perturbation theory arising from all levels. Following Ref. 12 we can write the single-mode relaxation rate off the 0 level as

$$\tau_{\text{el}}^{-1}(0,0)=\frac{n_{\text{ex}}f_0(T)\omega_{q\lambda}^4}{\pi\rho^2v_\lambda^2}\times\sum_{\lambda'}\frac{1}{v_{\lambda'}^5}\left[\sum_{m=1}^{3}\frac{(\Delta_{m0})^2\langle(M_{m0}^{q\lambda})^2\rangle\langle(M_{0m}^{q'\lambda'})^2\rangle}{\{(\hbar\omega_{q\lambda})^2-\Delta_{m0}^2\}^2+4\Delta_{m0}^2\Gamma_{m0}^2}\right], \tag{5}$$

where (0,0) represents the process for which both initial and final states are 0 states, and $M_{mn}^{q\lambda}=\sum_{j=1}^{4}f_j\Xi_{j\lambda}\alpha_j^m\alpha_j^n$, where

$$f_j=\left[1+\left[\frac{qa}{2}\right]^2-(a^2-b^2)\frac{q^2\cos^2\theta_j}{4}\right]^{-2};$$

θ_j is the angle between $\bar{q}$ and the z_j axis, the z_j axis is defined as being from the origin to the jth minimum of the conduction band, and a and b are the transverse and longitudinal Bohr radii, respectively. Values of $\Xi_{j\lambda}$ for different values of j and λ are given in Table II.

In a similar way we can obtain $\tau_{\text{el}}^{-1}(1,1)$, $\tau_{\text{el}}^{-1}(2,2)$, and $\tau_{\text{el}}^{-1}(3,3)$ as

$$\tau_{\text{el}}^{-1}(1,1)=\frac{n_{\text{ex}}f_1(T)\omega_{q\lambda}^4}{\pi\rho^2v_\lambda^2}\times\sum_{\lambda'}\frac{1}{v_{\lambda'}^5}\left[\sum_{\substack{n,m=0,3\\ n\neq m}}\left\{\frac{\Delta_{1m}^2\langle(M_{1m}^{q\lambda})^2\rangle\langle(M_{m1}^{q'\lambda'})^2\rangle}{\{(\hbar\omega_{q\lambda})^2-\Delta_{1m}^2\}^2+4\Delta_{1m}^2\Gamma_{1m}^2}+\frac{\Delta_{1m}\Delta_{1n}\langle(M_{1}^{q'\lambda}M_{n}^{q'\lambda'})\rangle\langle(M_{1m}^{q\lambda}M_{n1}^{q\lambda})\rangle\{(\hbar\omega_{q\lambda})^2-\Delta_{1m}^2\}\{(\hbar\omega_{q\lambda})^2-\Delta_{1n}^2\}}{\{(\hbar\omega_{q\lambda})^2-\Delta_{1m}^2\}\{(\hbar\omega_{q\lambda})^2-\Delta_{1n}^2\}+4[\Delta_{1n}^2\Gamma_{1n}^2\{(\hbar\omega_{q\lambda})^2-\Delta_{1m}^2\}^2+\Delta_{1m}^2\Gamma_{1m}^2\{(\hbar\omega_{q\lambda})^2-\Delta_{1n}^2\}^2+2\{(\hbar\omega_{q\lambda})^2-\Delta_{1m}^2\}\{(\hbar\omega_{q\lambda})^2-\Delta_{1n}^2\}\Delta_{1m}\Delta_{1n}\Gamma_{1m}\Gamma_{1n}]}\right\}\right], \tag{6}$$

$$\tau_{\text{el}}^{-1}(2,2)=\frac{n_{\text{ex}}f_2(T)\omega_{\lambda}^4}{\pi\rho^2v_\lambda^2}\times\sum_{\lambda'}\frac{1}{v_{\lambda'}^5}\left[\sum_{\substack{m,n=0,3\\ m\neq n}}\left\{\frac{|\Delta_{2m}|^2\langle(M_{m2}^{q'\lambda'})^2\rangle\langle(M_{2m}^{q\lambda})^2\rangle}{\{(\hbar\omega_{q\lambda})^2-|\Delta_{2m}|^2\}^2+4|\Delta_{2m}|^2\Gamma_{2m}^2}-\frac{|\Delta_{2m}||\Delta_{n2}|\langle(M_{m2}^{q\lambda'}M_{2n}^{q\lambda'})\rangle\langle(M_{2m}^{q\lambda}M_{n2}^{q\lambda})\rangle\{(\hbar\omega_{q\lambda})^2-|\Delta_{2m}|^2\}\{(\hbar\omega_{q\lambda})^2-|\Delta_{n2}|^2\}}{\{(\hbar\omega_{q\lambda})^2-|\Delta_{2m}|^2\}^2\{(\hbar\omega_{q\lambda})^2-|\Delta_{n2}|^2\}^2+4[|\Delta_{n2}|^2\Gamma_{n2}^2\{(\hbar\omega_{q\lambda})^2-|\Delta_{2m}|^2\}^2+|\Delta_{2m}|^2\Gamma_{2m}^2\{(\hbar\omega_{q\lambda})^2-|\Delta_{n2}|^2\}^2+2\{(\hbar\omega_{q\lambda})^2-|\Delta_{n2}|^2\}\{(\hbar\omega_{q\lambda})^2-|\Delta_{2m}|^2\}|\Delta_{2m}||\Delta_{n2}|\Gamma_{2m}\Gamma_{2n}]}\right\}\right], \tag{7}$$

$$\tau_{\rm el}^{-1}(3,3)=\frac{n_{\rm ex}f_3(T)\omega_q^4\lambda}{\pi\rho^2 v_\lambda^2}\sum_{\lambda'}\frac{1}{v_{\lambda'}^5}\left[\sum_{m=0,1,2}\frac{|\Delta_{3m}|^2\langle(M_{m3}^{q'\lambda'})^2\rangle\langle(M_{3m}^{q\lambda})^2\rangle}{\{(\hbar\omega_{q\lambda})^2-|\Delta_{3m}|^2\}^2+4|\Delta_{3m}|^2\Gamma_{3m}^2}\right], \tag{8}$$

and

$$\tau_{e\text{-ph}}^{-1}(\text{el})=\tau_{\rm el}^{-1}(0,0)+\tau_{\rm el}^{-1}(1,1)+\tau_{\rm el}^{-1}(2,2)+\tau_{\rm el}^{-1}(3,3)\ . \tag{9}$$

2. *Inelastic scattering*

These processes are

$$1s(n)+\hbar\omega_{q\lambda}\rightleftharpoons\text{Int.},\quad 1s(m)\rightleftharpoons 1s(n')+\hbar\omega_{q'\lambda'}\ ,$$

$E_{n'}$ being less than E_n. Here complication is much increased as compared to the unstressed sample because the energy of the intermediate state may even be higher than the initial state. This would introduce some terms in the matrix element which ultimately cause a singularity in the transition probability for a particular value of $\omega_{q\lambda}$ if appropriate level width is not added in their denominator. We, for consistency with the treatment given in elastic scattering, adopt the scheme given by Heitler.[13] For example, the transition probability for the process (2,0) is

$$\begin{aligned}W_{20}(q\lambda\rightarrow q'\lambda')n_{q\lambda}(1+n_{q'\lambda'})=&\frac{2\pi}{\hbar^2}\delta\left[\omega_{q'\lambda'}-\left[\omega_{q\lambda}+\frac{\Delta_{20}}{\hbar}\right]\right]f_2(T)\\&\times\left|-\frac{M_{02}^{q'\lambda'}M_{22}^{q'\lambda'}}{\hbar\omega_{q\lambda}+i\Gamma_2}+\frac{M_{02}^{q\lambda}M_{22}^{q'\lambda'}}{\hbar\omega_{q\lambda}+\Delta_{20}-i\Gamma_2}-\frac{M_{00}^{q'\lambda'}M_{02}^{q\lambda}}{\hbar\omega_{q\lambda}+\Delta_{20}-i\Gamma_0}+\frac{M_{00}^{q\lambda}M_{02}^{q'\lambda'}}{\hbar\omega_{q\lambda}-i\Gamma_0}\right.\\&\left.-\frac{M_{03}^{q'\lambda'}M_{32}^{q\lambda}}{\hbar\omega_{q\lambda}-\Delta_{32}+i\Gamma_3}+\frac{M_{03}^{q\lambda}M_{32}^{q'\lambda'}}{\hbar\omega_{q\lambda}+\Delta_{30}-i\Gamma_3}\right|^2(a_{q'\lambda'}^*a_{q\lambda})^2q^2q'^2\ .\end{aligned} \tag{10a}$$

To avoid the pseudoresonance of the fifth term, we have added level width Γ_3 in it. In Eq. (10a) all terms other than the said one will not contribute significantly to the transition probability. So, such terms can be neglected. Thus finally we get

$$\begin{aligned}\tau_{\rm inel}^{-1}(2,0)\approx&\frac{n_{\rm ex}f_2(T)\omega_{q\lambda}}{4\pi\rho^2v_\lambda^2}\sum_{\lambda'}\frac{(\Delta_{20}/\hbar+\omega_{q\lambda})^3}{v_{\lambda'}^5}\left[\frac{\langle(M_{03}^{q'\lambda'})^2\rangle\langle(M_{32}^{q\lambda})^2\rangle}{(\hbar\omega_{q\lambda}-\Delta_{32})^2+\Gamma_3^2}\right]\left[1-\exp\left[-\frac{\hbar\omega_{q\lambda}}{k_BT}\right]\right]\\&\times\left[1-\exp\left[\frac{-\Delta_{20}-\hbar\omega_{q\lambda}}{k_BT}\right]\right]^{-1}.\end{aligned} \tag{10b}$$

Similarly we can find the expressions for $\tau_{\rm inel}^{-1}(3,0)$ and $\tau_{\rm inel}^{-1}(1,2)$:

$$\begin{aligned}\tau_{\rm inel}^{-1}(3,0)\approx&\frac{n_{\rm ex}f_3(T)\omega_{q\lambda}}{4\pi\rho^2v_\lambda^2}\sum_{\lambda'}\frac{(\Delta_{30}/\hbar+\omega_{q\lambda})^3}{v_{\lambda'}^5}\left[\frac{\langle(M_{01}^{q'\lambda'})^2\rangle\langle(M_{31}^{q\lambda})^2\rangle}{(\hbar\omega_{q\lambda}-\Delta_{13})^2+\Gamma_1^2}-\frac{2\{(\hbar\omega_{q\lambda}-\Delta_{13})+\Gamma_1\}\langle(M_{01}^{q'\lambda'}M_{13}^{q'\lambda'})\rangle\langle(M_{31}^{q\lambda}M_{10}^{q\lambda})\rangle}{\{(\hbar\omega_{q\lambda}-\Delta_{13})^2+\Gamma_1^2\}\{\hbar\omega_{q\lambda}+\Delta_{10}\}}\right]\\&\times\left[1-\exp\left[-\frac{\hbar\omega_{q\lambda}}{k_BT}\right]\right]\left[1-\exp\left[\frac{-\Delta_{30}-\hbar\omega_{q\lambda})}{k_BT}\right]\right]^{-1},\end{aligned} \tag{11}$$

$$\begin{aligned}\tau_{\rm inel}^{-1}(1,2)\approx&\frac{n_{\rm ex}f_1(T)\omega_{q\lambda}}{4\pi\rho^2v_\lambda^2}\sum_{\lambda'}\frac{(\Delta_{12}/\hbar+\omega_{q\lambda})^3}{v_{\lambda'}^5}\left[\frac{\langle(M_{20}^{q\lambda})^2\rangle\langle(M_{01}^{q'\lambda'})^2\rangle}{(\hbar\omega_{q\lambda}-\Delta_{20})^2+\Gamma_0^2}+\frac{2\{(\hbar\omega_{q\lambda}-\Delta_{20})+\Gamma_0\}\langle(M_{32}^{q\lambda}M_{20}^{q\lambda})\rangle\langle(M_{13}^{q'\lambda'}M_{01}^{q'\lambda'})\rangle}{(\hbar\omega_{q\lambda}+\Delta_{32})\{(\hbar\omega_{q\lambda}-\Delta_{20})^2+\Gamma_0^2\}}\right]\\&\times\left[1-\exp\left[-\frac{\hbar\omega_{q\lambda}}{k_BT}\right]\right]\left[1-\exp\left[\frac{-\Delta_{12}-\hbar\omega_{q\lambda}}{k_BT}\right]\right]^{-1}.\end{aligned} \tag{12}$$

Also, for

$$\begin{aligned}\tau_{\rm inel}^{-1}(3,2)\approx&\frac{n_{\rm ex}f_3(T)\omega_{q\lambda}}{4\pi\rho^2v_\lambda^2}\sum_{\lambda'}\frac{(\Delta_{32}/\hbar+\omega_{q\lambda})^3}{v_{\lambda'}^5}\left[\frac{\langle(M_{20}^{q\lambda})^2\rangle\langle(M_{03}^{q'\lambda'})^2\rangle}{(\hbar\omega_{q\lambda}-\Delta_{20})^2+\Gamma_0^2}\right]\left[1-\exp\left[-\frac{\hbar\omega_{q\lambda}}{k_BT}\right]\right]\\&\times\left[1-\exp\left[\frac{-\Delta_{32}-\hbar\omega_{q\lambda}}{k_BT}\right]\right]^{-1},\end{aligned} \tag{13}$$

$$\tau_{\text{inel}}^{-1}(1,3)\approx\frac{n_{\text{ex}}f_1(T)\omega_{q\lambda}}{4\pi\rho^2v_\lambda^2}\sum_{\lambda'}\frac{(\Delta_{13}/\hbar+\omega_{q\lambda})^3}{v_{\lambda'}^5}\left[\frac{\langle(M_{30}^{q\lambda})^2\rangle\langle(M_{01}^{q'\lambda'})^2\rangle}{(\hbar\omega_{q\lambda}-\Delta_{30})^2+\Gamma_0^2}\right]\left[1-\exp\left[-\frac{\hbar\omega_{q\lambda}}{k_BT}\right]\right]\times\left[1-\exp\left[\frac{-\Delta_{13}-\hbar\omega_{q\lambda}}{k_BT}\right]\right]^{-1}. \tag{14}$$

The $\tau_{\text{inel}}^{-1}(1,0)$ process can be neglected.

Finally, we can write

$$\tau_{e\text{-ph}}^{-1}(\text{inel})=\tau_{\text{inel}}^{-1}(2,0)+\tau_{\text{inel}}^{-1}(3,0)+\tau_{\text{inel}}^{-1}(1,2)+\tau_{\text{inel}}^{-1}(3,2)+\tau_{\text{inel}}^{-1}(1,3)\ . \tag{15}$$

3. *Absorption processes*

These can be summarized as

$$1s(n)+\hbar\omega_{q'\lambda'}+\hbar\omega_{q\lambda}\rightleftharpoons\text{Int.},\quad 1s(m)\rightleftharpoons 1s(n')\ ,$$

$E_{n'}>E_n$. Here, pseudoresonances would appear in the transition probability due to the intermediate states, for which E_m is different both from E_n and $E_{n'}$. To avoid these resonances we once again follow Heitler's[13] technique to add level width in the denominator. In order to maintain the consistency the same method is employed also near the actual resonance where $\hbar\omega_{q\lambda}=E_{n'}-E_n$. Through similar approximations used in the preceding section, we can write the thermally assisted phonon absorption relaxation rate for different transitions as

$$\tau_{\text{ab}}^{-1}(0,2)\approx\frac{n_{\text{ex}}f_0(T)\omega_{q\lambda}}{4\pi\rho^2v_\lambda^2}\sum_{\lambda'}\frac{|\Delta_{20}/\hbar-\omega_{q\lambda}|^3}{v_{\lambda'}^5}\left[\langle(M_{20}^{q\lambda})^2\rangle\left[\frac{\langle(M_{00}^{q'\lambda'})^2\rangle}{(\hbar\omega_{q\lambda}-\Delta_{20})^2+\Gamma_0^2}+\frac{\langle(M_{22}^{q'\lambda'})^2\rangle}{(\hbar\omega_{q\lambda}-\Delta_{20})^2+\Gamma_2^2}-2\frac{\langle(M_{22}^{q'\lambda'}M_{00}^{q'\lambda'})\rangle\{(\hbar\omega_{q\lambda}-\Delta_{20})^2+\Gamma_0\Gamma_2\}}{\{(\hbar\omega_{q\lambda}-\Delta_{20})^2+\Gamma_0^2\}\{(\hbar\omega_{q\lambda}-\Delta_{20})^2+\Gamma_2^2\}}\right]+\frac{\langle(M_{23}^{q'\lambda'})^2\rangle\langle(M_{30}^{q\lambda})^2\rangle}{(\hbar\omega_{q\lambda}-\Delta_{30})^2+\Gamma_3^2}\right]\left[1-\exp\left[-\frac{\hbar\omega_{q\lambda}}{k_BT}\right]\right]\times\left[\left|\exp\left[\frac{\Delta_{20}-\hbar\omega_{q\lambda}}{k_BT}\right]-1\right|\right]^{-1}, \tag{16}$$

$$\begin{aligned}\tau_{\text{ab}}^{-1}(0,3)\approx&\frac{n_{\text{ex}}f_0(T)\omega_{q\lambda}}{4\pi\rho^2v_\lambda^2}\sum_{\lambda'}\frac{|\Delta_{30}/\hbar-\omega_{q\lambda}|^3}{v_{\lambda'}^5}\\&\times\left[\langle(M_{30}^{q\lambda})^2\rangle\left[\frac{\langle(M_{00}^{q'\lambda'})^2\rangle}{(\hbar\omega_{q\lambda}-\Delta_{30})^2+\Gamma_0^2}+\frac{\langle(M_{33}^{q'\lambda'})^2\rangle}{(\hbar\omega_{q\lambda}-\Delta_{30})^2+\Gamma_3^2}-2\frac{\langle(M_{00}^{q'\lambda'}M_{33}^{q'\lambda'})\rangle\{(\hbar\omega_{q\lambda}-\Delta_{30})^2+\Gamma_0\Gamma_3\}}{\{(\hbar\omega_{q\lambda}-\Delta_{30})^2+\Gamma_0^2\}\{(\hbar\omega_{q\lambda}-\Delta_{30})^2+\Gamma_3^2\}}\right]\\&+\frac{\langle(M_{23}^{q'\lambda'})^2\rangle\langle(M_{20}^{q\lambda})^2\rangle}{\{(\hbar\omega_{q\lambda}-\Delta_{20})^2+\Gamma_2^2\}}+\frac{\langle(M_{32}^{q\lambda})^2\rangle\langle(M_{02}^{q'\lambda'})^2\rangle}{(\hbar\omega_{q\lambda}-\Delta_{32})^2+\Gamma_2^2}\\&-2\frac{\langle(M_{23}^{q'\lambda'}M_{02}^{q'\lambda'})\rangle\langle(M_{20}^{q\lambda}M_{32}^{q\lambda})\rangle\{(\hbar\omega_{q\lambda}-\Delta_{20})(\hbar\omega_{q\lambda}-\Delta_{32})+\Gamma_2^2\}}{\{(\hbar\omega_{q\lambda}-\Delta_{20})^2+\Gamma_2^2\}\{(\hbar\omega_{q\lambda}-\Delta_{32})^2+\Gamma_2^2\}}\\&+\frac{\langle(M_{13}^{q'\lambda'})^2\rangle\langle(M_{10}^{q\lambda})^2\rangle}{\{(\hbar\omega_{q\lambda}-\Delta_{10})^2+\Gamma_1^2\}}\\&-2\frac{\langle(M_{13}^{q'\lambda'}M_{01}^{q'\lambda'})\rangle\langle(M_{10}^{q\lambda}M_{31}^{q\lambda})\rangle\{(\hbar\omega_{q\lambda}-\Delta_{10})+\Gamma_1\}}{\{(\hbar\omega_{q\lambda}-\Delta_{10})^2+\Gamma_1^2\}\{\hbar\omega_{q\lambda}+\Delta_{13}\}}\Bigg]\\&\times\left[1-\exp\left[-\frac{\hbar\omega_{q\lambda}}{k_BT}\right]\right]\left[\left|\exp\left[\frac{\Delta_{30}-\hbar\omega_{q\lambda}}{k_BT}\right]-1\right|\right]^{-1},\end{aligned} \tag{17}$$

$$\tau_{ab}^{-1}(0,1)=\frac{n_{ex}f_0(T)\omega_{q\lambda}}{4\pi\rho^2 v_\lambda^2}\sum_{\lambda'}\frac{|\Delta_{10}/\hbar-\omega_{q\lambda}|^3}{v_{\lambda'}^5}$$
$$\times\left[\langle(M_{10}^{q\lambda})^2\rangle\left\{\frac{\langle(M_{00}^{q'\lambda'})^2\rangle}{(\hbar\omega_{q\lambda}-\Delta_{10})^2+\Gamma_0^2}+\frac{\langle(M_{11}^{q'\lambda'})^2\rangle}{(\hbar\omega_{q\lambda}-\Delta_{10})^2+\Gamma_1^2}\right.\right.$$
$$\left.-2\frac{\langle(M_{00}^{q'\lambda'}M_{11}^{q'\lambda'})\rangle\{(\hbar\omega_{q\lambda}-\Delta_{10})^2+\Gamma_0\Gamma_1\}}{\{(\hbar\omega_{q\lambda}-\Delta_{10})^2+\Gamma_0^2\}\{(\hbar\omega_{q\lambda}-\Delta_{10})^2+\Gamma_1^2\}}\right\]$$
$$+\frac{\langle(M_{13}^{q'\lambda'})^2\rangle\langle(M_{30}^{q\lambda})^2\rangle}{(\hbar\omega_{q\lambda}-\Delta_{30})^2+\Gamma_3^2}+\frac{\langle(M_{31}^{q\lambda})^2\rangle\langle(M_{03}^{q'\lambda'})^2\rangle}{(\hbar\omega_{q\lambda}-\Delta_{13})^2+\Gamma_3^2}\Bigg]$$
$$\times\left[1-\exp\left[-\frac{\hbar\omega_{q\lambda}}{k_BT}\right]\right]\left[\left|\exp\left[\frac{\Delta_{10}-\hbar\omega_{q\lambda}}{k_BT}\right]-1\right|\right]^{-1}, \tag{18}$$

$$\tau_{ab}^{-1}(2,1)=\frac{n_{ex}f_2(T)\omega_{q\lambda}}{4\pi\rho^2 v_\lambda^2}\sum_{\lambda'}\frac{|\Delta_{12}/\hbar-\omega_{q\lambda}|^3}{v_{\lambda'}^5}$$
$$\times\left[\frac{\langle(M_{13}^{q'\lambda'})^2\rangle\langle(M_{32}^{q\lambda})^2\rangle}{(\hbar\omega_{q\lambda}-\Delta_{32})^2+\Gamma_3^2}+\frac{\langle(M_{10}^{q\lambda})^2\rangle\langle(M_{02}^{q'\lambda'})^2\rangle}{(\hbar\omega_{q\lambda}-\Delta_{10})^2+\Gamma_0^2}+\frac{\langle(M_{31}^{q\lambda})^2\rangle\langle(M_{23}^{q'\lambda'})^2\rangle}{(\hbar\omega_{q\lambda}-\Delta_{13})^2+\Gamma_3^2}\right.$$
$$+\frac{2\langle(M_{01}^{q'\lambda'}M_{13}^{q'\lambda'})\rangle\langle(M_{20}^{q\lambda}M_{32}^{q\lambda})\rangle\{\hbar\omega_{q\lambda}-\Delta_{32})+\Gamma_3\}}{(\hbar\omega_{q\lambda}+\Delta_{20})\{(\hbar\omega_{q\lambda}-\Delta_{32})^2+\Gamma_3^2\}}$$
$$\left.+\frac{2\{(\hbar\omega_{q\lambda}-\Delta_{10})(\hbar\omega_{q\lambda}-\Delta_{13})+\Gamma_0\Gamma_3\}\langle(M_{10}^{q\lambda}M_{31}^{q\lambda})\rangle\langle(M_{02}^{q'\lambda'}M_{23}^{q'\lambda'})\rangle}{\{(\hbar\omega_{q\lambda}-\Delta_{10})^2+\Gamma_0^2\}\{(\hbar\omega_{q\lambda}-\Delta_{13})^2+\Gamma_3^2\}}\right]$$
$$\times\left[1-\exp\left[-\frac{\hbar\omega_{q\lambda}}{k_BT}\right]\right]\left[\left|\exp\left[\frac{\Delta_{12}-\hbar\omega_{q\lambda}}{k_BT}\right]-1\right|\right]^{-1}, \tag{19}$$

$$\tau_{ab}^{-1}(2,3)=\frac{n_{ex}f_2(T)\omega_{q\lambda}}{4\pi\rho^2 v_\lambda^2}\sum_{\lambda'}\frac{|\Delta_{32}/\hbar-\omega_{q\lambda}|^3}{v_{\lambda'}^5}$$
$$\times\left[\langle(M_{32}^{q\lambda})^2\rangle\left\{\frac{\langle(M_{22}^{q'\lambda'})^2\rangle}{\{(\hbar\omega_{q\lambda}-\Delta_{32})^2+\Gamma_2^2\}}+\frac{\langle(M_{33}^{q'\lambda'})^2\rangle}{\{(\hbar\omega_{q\lambda}-\Delta_{32})^2+\Gamma_3^2\}}\right.\right.$$
$$\left.-2\frac{\langle(M_{22}^{q'\lambda'}M_{33}^{q'\lambda'})\rangle\{(\hbar\omega_{q\lambda}-\Delta_{32})^2+\Gamma_2\Gamma_3\}}{\{(\hbar\omega_{q\lambda}-\Delta_{32})^2+\Gamma_2^2\}\{(\hbar\omega_{q\lambda}-\Delta_{32})^2+\Gamma_3^2\}}\right\]$$
$$+\frac{\langle(M_{30}^{q\lambda})^2\rangle\langle(M_{02}^{q'\lambda'})^2\rangle}{\{(\hbar\omega_{q\lambda}-\Delta_{30})^2+\Gamma_0^2\}}\Bigg]\left[1-\exp\left[-\frac{\hbar\omega_{q\lambda}}{k_BT}\right]\right]\left[\left|\exp\left[\frac{\Delta_{32}-\hbar\omega_{q\lambda}}{k_BT}\right]-1\right|\right]^{-1}, \tag{20}$$

$$\tau_{ab}^{-1}(3,1)=\frac{n_{ex}f_3(T)\omega_{q\lambda}}{4\pi\rho^2 v_\lambda^2}\sum_{\lambda'}\frac{|\Delta_{13}/\hbar-\omega_{q\lambda}|^3}{v_{\lambda'}^5}$$
$$\times\left[\langle(M_{31}^{q\lambda})^2\rangle\left\{\frac{\langle(M_{33}^{q'\lambda'})^2\rangle}{\{(\hbar\omega_{q\lambda}-\Delta_{13})^2+\Gamma_3^2\}}+\frac{\langle(M_{11}^{q'\lambda'})^2\rangle}{\{(\hbar\omega_{q\lambda}-\Delta_{13})^2+\Gamma_1^2\}}\right.\right.$$
$$\left.-2\frac{\langle(M_{33}^{q'\lambda'}M_{11}^{q'\lambda'})\rangle\{(\hbar\omega_{q\lambda}-\Delta_{13})^2+\Gamma_1\Gamma_3\}}{\{(\hbar\omega_{q\lambda}-\Delta_{13})^2+\Gamma_3^2\}\{(\hbar\omega_{q\lambda}-\Delta_{13})^2+\Gamma_1^2\}}\right\]$$
$$+\frac{\langle(M_{10}^{q\lambda})^2\rangle\langle(M_{03}^{q'\lambda'})^2\rangle}{\{(\hbar\omega_{q\lambda}-\Delta_{10})^2+\Gamma_0^2\}}\Bigg]\left[1-\exp\left[-\frac{\hbar\omega_{q\lambda}}{k_BT}\right]\right]\left[\left|\exp\left[\frac{\Delta_{13}-\hbar\omega_{q\lambda}}{k_BT}\right]-1\right|\right]^{-1}. \tag{21}$$

Near true resonance, these expressions cannot be used as they become zero due to the factor $|\Delta-\hbar\omega_{q\lambda}|^3$ in the numerator. On adding the level width with Δ, however, near resonance the expressions from Eqs. (16)–(21) can be approximated to the following forms:

$$\tau_{ab}^{-1}(0,2)=\frac{n_{ex}f_0(T)\omega_{q\lambda}}{4\pi\rho^2 v_\lambda^2}\sum_{\lambda'}\frac{1}{v_{\lambda'}^5}\left[\frac{k_BT}{\hbar^3}\right][\langle(M_{20}^{q\lambda})^2\rangle\{\langle(M_{00}^{q'\lambda'})^2\rangle+\langle(M_{22}^{q'\lambda'})^2\rangle-2\langle(M_{22}^{q'\lambda'}M_{00}^{q'\lambda'})\rangle\}]$$
$$\times\left[1-\exp\left[-\frac{\hbar\omega_{q\lambda}}{k_BT}\right]\right], \tag{16'}$$

$$\tau_{ab}^{-1}(0,3)=\frac{n_{ex}f_0(T)\omega_{q\lambda}}{4\pi\rho^2 v_\lambda^2}\sum_{\lambda'}\frac{1}{v_{\lambda'}^5}\left[\frac{k_BT}{\hbar^3}\right][\langle(M_{30}^{q\lambda})^2\rangle\{\langle(M_{00}^{q'\lambda'})^2\rangle+\langle(M_{33}^{q'\lambda'})^2\rangle-2\langle(M_{00}^{q'\lambda'}M_{33}^{q'\lambda'})\rangle\}]$$
$$\times\left[1-\exp\left[-\frac{\hbar\omega_{q\lambda}}{k_BT}\right]\right], \tag{17'}$$

$$\tau_{ab}^{-1}(0,1)=\frac{n_{ex}f_0(T)\omega_{q\lambda}}{4\pi\rho^2 v_{\lambda'}^2}\sum_{\lambda'}\frac{1}{v_{\lambda'}^5}\left[\frac{k_BT}{\hbar^3}\right][\langle(M_{10}^{q\lambda})^2\rangle\{\langle(M_{00}^{q'\lambda'})^2\rangle+\langle(M_{11}^{q'\lambda'})^2\rangle-2\langle(M_{00}^{q'\lambda'}M_{11}^{q'\lambda'})\rangle\}]$$
$$\times\left[1-\exp\left[-\frac{\hbar\omega_{q\lambda}}{k_BT}\right]\right], \tag{18'}$$

$\tau_{ab}^{-1}(2,1)=0$; as the matrix element for 2 to 1 transition is zero . (19')

$$\tau_{ab}^{-1}(2,3)=\frac{n_{ex}f_2(T)\omega_{q\lambda}}{4\pi\rho^2 v_\lambda^2}\sum_{\lambda'}\frac{1}{v_{\lambda'}^5}\left[\frac{k_BT}{\hbar^3}\right][\langle(M_{32}^{q\lambda})^2\rangle\{\langle(M_{22}^{q'\lambda'})^2\rangle+\langle(M_{33}^{q'\lambda'})^2\rangle-2\langle(M_{22}^{q'\lambda'}M_{33}^{q'\lambda'})\rangle\}]$$
$$\times 1-\exp\left[-\frac{\hbar\omega_{q\lambda}}{k_BT}\right]\Bigg], \tag{20'}$$

$$\tau_{ab}^{-1}(3,1)=\frac{n_{ex}f_3(T)\omega_{q\lambda}}{4\pi\rho^2 v_\lambda^2}\sum_{\lambda'}\frac{1}{v_{\lambda'}^5}\left[\frac{k_BT}{\hbar^3}\right][\langle(M_{31}^{q\lambda})^2\rangle\{\langle(M_{33}^{q'\lambda'})^2\rangle+\langle(M_{11}^{q'\lambda'})^2\rangle-2\langle(M_{33}^{q'\lambda'}M_{11}^{q'\lambda'})\rangle\}]$$
$$\times\left[1-\exp\left[-\frac{\hbar\omega_{q\lambda}}{k_BT}\right]\right]. \tag{21'}$$

It should be remarked that near resonance, Green's function technique should be employed to calculate τ_{ab}^{-1}. In the absence of such expression for the nondegenerate four-level system and to maintain consistency with the rest of the mathematical treatment we have used the above written approximate expressions only.

The total relaxation rate due to the thermally assisted phonon absorption process is

$$\tau_{e\text{-ph}}^{-1}(ab)=\tau_{ab}^{-1}(0,2)+\tau_{ab}^{-1}(0,3)+\tau_{ab}^{-1}(0,1)+\tau_{ab}^{-1}(2,1)+\tau_{ab}^{-1}(2,3)+\tau_{ab}^{-1}(3,1)\ . \tag{22}$$

Following Kowk[14] we obtain the level widths for 0, 1, 2, and 3 levels as follows:

$$\Gamma_0=\frac{1}{4\pi\rho}\sum_\lambda\frac{1}{v_\lambda^5}\left\{\left[\frac{\Delta_{20}}{\hbar}\right]^3\langle(M_{20}^{q\lambda})^2\rangle\left[\exp\left[\frac{\Delta_{20}}{k_BT}\right]-1\right]^{-1}+\left[\frac{\Delta_{30}}{\hbar}\right]^3\langle(M_{30}^{q\lambda})^2\rangle\left[\exp\left[\frac{\Delta_{30}}{k_BT}\right]-1\right]^{-1}\right.$$
$$\left.+\left[\frac{\Delta_{10}}{\hbar}\right]^3\langle(M_{10}^{q\lambda})^2\rangle\left[\exp\left[\frac{\Delta_{10}}{k_BT}\right]-1\right]^{-1}\right\}, \tag{23}$$

$$\Gamma_1=\frac{1}{4\pi\rho}\sum_\lambda\frac{1}{v_\lambda^5}\left\{\left[\frac{\Delta_{10}}{\hbar}\right]^3\langle(M_{10}^{q\lambda})^2\rangle\left[1-\exp\left[-\frac{\Delta_{10}}{k_BT}\right]\right]^{-1}\right.$$
$$\left.+\left[\frac{\Delta_{12}}{\hbar}\right]^3\langle(M_{12}^{q\lambda})^2\rangle\left[1-\exp\left[-\frac{\Delta_{12}}{k_BT}\right]\right]^{-1}+\left[\frac{\Delta_{13}}{\hbar}\right]^3\langle(M_{13}^{q\lambda})^2\rangle\left[1-\exp\left[-\frac{\Delta_{13}}{k_BT}\right]\right]^{-1}\right\}, \tag{24}$$

$$\Gamma_2=\frac{1}{4\pi\rho}\sum_\lambda\frac{1}{v_\lambda^5}\left\{\left[\frac{\Delta_{20}}{\hbar}\right]^3\langle(M_{20}^{q\lambda})^2\rangle\left[1-\exp\left[-\frac{\Delta_{20}}{k_BT}\right]\right]^{-1}+\left[\frac{\Delta_{32}}{\hbar}\right]^3\langle(M_{32}^{q\lambda})^2\rangle\left[\exp\left[\frac{\Delta_{32}}{k_BT}\right]-1\right]^{-1}\right\}, \tag{25}$$

$$\Gamma_3=\frac{1}{4\pi\rho}\sum_\lambda\frac{1}{v_\lambda^5}\left\{\left[\frac{\Delta_{30}}{\hbar}\right]^3\langle(M_{30}^{q\lambda})^2\rangle\left[1-\exp\left[-\frac{\Delta_{30}}{k_BT}\right]\right]^{-1}\right.$$
$$\left.+\left[\frac{\Delta_{32}}{\hbar}\right]^3\langle(M_{32}^{q\lambda})^2\rangle\left[1-\exp\left[-\frac{\Delta_{32}}{k_BT}\right]\right]^{-1}+\left[\frac{\Delta_{13}}{\hbar}\right]^3\langle(M_{13}^{q\lambda})^2\rangle\left[\exp\left[\frac{\Delta_{13}}{k_BT}\right]-1\right]^{-1}\right\}. \tag{26}$$

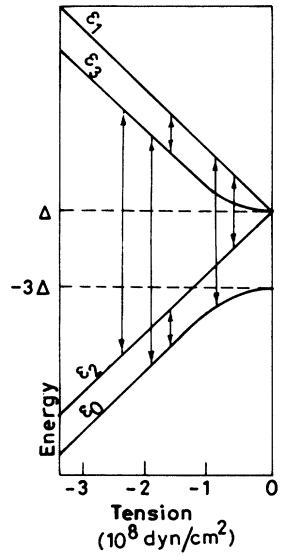

FIG. 1. The energy of the four 1*s*-like donor states in *n*-type Ge when uniaxial stress (tension) is applied in the [110] direction.

TABLE II. Value of $\Xi_{j\lambda}$ for different values of j and λ.

$$\Xi_{11}=E_d+\left[\frac{E_u}{3}\right](1+\sin^2\theta\sin2\phi+\sin2\theta\sin\phi+\sin2\theta\cos\phi)$$

$$\Xi_{12}=\frac{E_u}{3}(\tfrac{1}{2}\sin2\theta\sin2\phi+\cos2\theta\cos\phi+\cos2\theta\sin\phi)$$

$$\Xi_{13}=\frac{E_u}{3}(\sin\theta\cos2\phi-\cos\theta\sin\phi+\cos\theta\cos\phi)$$

$$\Xi_{21}=E_d+\frac{E_u}{3}(1-\sin^2\theta\sin2\phi-\sin2\theta\cos\phi+\sin2\theta\sin\phi)$$

$$\Xi_{22}=\frac{E_u}{3}(-\tfrac{1}{2}\sin2\theta\sin2\phi+\cos2\theta\sin\phi-\cos2\theta\cos\phi)$$

$$\Xi_{23}=\frac{E_u}{3}(\cos\theta\sin\phi+\cos\theta\cos\phi-\sin\theta\cos2\phi)$$

$$\Xi_{31}=E_d+\frac{E_u}{3}(1+\sin^2\theta\sin2\phi-\sin2\theta\cos\phi-\sin2\theta\sin\phi)$$

$$\Xi_{32}=\frac{E_u}{3}(\tfrac{1}{2}\sin2\theta\sin2\phi-\cos2\theta\cos\phi-\cos2\theta\sin\phi)$$

$$\Xi_{33}=\frac{E_u}{3}(\sin\theta\cos2\phi+\cos\theta\sin\phi-\cos\theta\cos\phi)$$

$$\Xi_{41}=E_d+\frac{E_u}{3}(1-\sin^2\theta\sin2\phi+\sin2\theta\cos\phi-\sin2\theta\sin\phi)$$

$$\Xi_{42}=\frac{E_u}{3}(-\tfrac{1}{2}\sin2\theta\sin2\phi+\cos2\theta\cos\phi-\cos2\theta\sin\phi)$$

$$\Xi_{43}=\frac{E_u}{3}(-\sin\theta\cos2\phi-\cos\theta\sin\phi-\cos\theta\cos\phi)$$

C. Phonon conductivity

According to Holland,[15] phonon conductivity $\kappa(T)$ can be written as

$$\kappa(T)=\frac{k_B^4T^3}{6\pi^2\hbar^3}\sum_{\lambda=1}^{3}\frac{1}{v_\lambda}\int_0^{\theta_D/T}\frac{x^4e^x}{(e^x-1)^2\tau^{-1}(x)}dx\ , \tag{27}$$

where $\lambda=1$ for longitudinal mode and $\lambda=2,3$ are for transverse modes. $x=(\hbar\omega_{q\lambda}/k_BT)$, k_B is the Boltzmann constant, v_λ the phonon velocity, and $\omega_{q\lambda}$ the phonon frequency. $\tau^{-1}=\tau_b^{-1}+\tau_{pt}^{-1}+\tau_{e\text{-ph}}^{-1}+\tau_{\text{ph-ph}}^{-1}$ is the total relaxation rates. $\tau_b^{-1}=v_\lambda/L_c$, L_c is the Casimir length; $\tau_{pt}^{-1}=A\omega_{q\lambda}^4$; $\tau_{e\text{-ph}}^{-1}=\tau_{e\text{-ph}}^{-1}(\text{el})+\tau_{e\text{-ph}}^{-1}(\text{inel})+\tau_{e\text{-ph}}^{-1}(\text{ab})$ is the total electron-phonon relaxation rate; $\tau_{\text{ph-ph}}^{-1}=B_l\omega_{q\lambda}^2T^3$ for longitudinal phonon and $\tau_{\text{ph-ph}}^{-1}=B_t\omega_{q\lambda}T^4$ for transverse phonon. Values of the parameters and physical constants used in this calculation are $\bar{v}_1=5.37\times10^5$ cm/sec, $\bar{v}_2=\bar{v}_3=3.28\times10^5$ cm/sec, $L_c=0.146$ cm, $A=5.10\times10^{-45}$ sec^3, $B_l=6.899\,74\times10^{-24}$ secK^{-3}, $B_t=1.0\times10^{-11}K^{-4}$, $\rho=5.35$ g/cm^3.

TABLE I. Parameters used for the calculations of electron-phonon relaxation rates.

n_{ex}	2.0×10^{16}/cm^3
4Δ	0.32 meV
a	6.9865×10^{-7} cm
b	1.5749×10^{-7} cm
E_d	-8.0 eV
E_{u0}	16.5 eV
η	$0.541\,66\times10^{-8}$ cm^2/dyn
μ	0.1×10^{-8} cm^2/dyn

III. RESULTS AND DISCUSSION

Our initial calculations of phonon resistivity versus stress at $T=2.82$ K with all relaxation rates derived in the preceding section show a small peak near $X=-1.25\times10^8$ dyn/cm^2 (see Fig. 2). For consistency, we preferred to use our present derived expressions at $X\to0$ also. For these calculations parameters used are given in the caption of Fig. 2. These parameters were obtained through the best computer fit of the phonon-

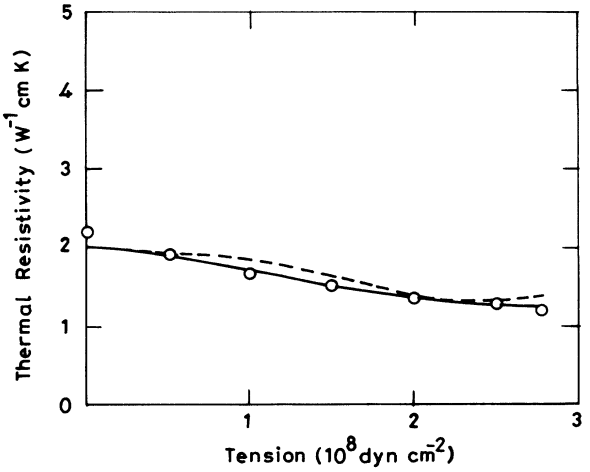

FIG. 2. Thermal resistivity vs tension at constant temperature, $T=2.82$ K for Sb-doped Ge. Solid line shows calculation for adjusted value of E_u and r; dashed line shows calculations for $\eta=0$, $\mu=0$, and $E_u=16.5$ eV; $E_d=-8$ eV; $A=5.10\times10^{-45}$ sec^3; $L_c=0.146$ cm; circles are the experimental points.

conductivity data without stress (see Fig. 3). Two important aspects which were not considered in these initial calculations are the following.

(i) Variation of the Bohr radii corresponding to various levels: The hydrogenlike envelope function, in fact, must be perturbed in the presence of stress. The effect of this perturbation may be seen through the change in Bohr radii. Fritzsche[9] reports that the tensile stress expands levels 1 and 3 and the other two levels are somewhat contracted. The variation in r with stress, however, is expected to be larger due to the dilatational effects[16,17] on the center of gravity of the conduction-band minima as well as donor states.

(ii) The effect of stress on E_u: According to the experimental observation of Tekippe *et al.*,[18] stress in [100] direction suggests that for n-type Si, E_u should slightly decrease with stress. We believe that the [110] stress which affects the thermal resistance much more than the [100] stress should have a larger influence on E_u.

To improvise the calculation, therefore, we have chosen the value of $E_u = E_{u0}(1-\eta|X|)$, E_{u0} being the zero stress value of the deformation potential. To incorporate the first aspect, the Bohr radii of the lower two levels (0 and 2) have been kept constant for convenience and taken equal to the mean Bohr radii r_0. Here r stands for both a and b, while for the upper two levels (1 and 3) we define $r_u = r_0(1+\mu|X|)$. μ and η are adjustable parameters. While calculating $\tau_{e\text{-ph}}^{-1}$ for transitions from the lower to upper levels we have[2] $2/r = 1/r_0 + 1/r_u$.

In Figs. 4(a), 4(b), and 4(c), we have plotted $\tau_{e\text{-ph}}^{-1}(\text{el})$, $\tau_{e\text{-ph}}^{-1}(\text{ab})$, τ_b^{-1}, and τ_{pt}^{-1} with ω for three values of tensile [110] stress at $T = 2.82$ K. $\tau_{e\text{-ph}}^{-1}(\text{inel})$ has been found to be negligible at this temperature. In the unstressed Sb-doped Ge the donor $1s$ state is a two-level system; hence only one peak in the $\tau_{e\text{-ph}}^{-1}$ vs ω curve appears at $\omega_r = 4.86\times10^{11}$ Hz. Under the [110] stress, the degeneracy of the triplet levels is lifted and six resonance peaks should appear in Fig. 4. Since some energy gaps are nearly equal, we can observe only two prominent peaks. It is obvious from Fig. 4 that for low and high values of stress, i.e., $|X| < 0.5\times10^8$ and $|X| > 1.5\times10^8$ dyn/cm^2, boundary scattering of phonons would be an important mechanism as there is a very large region of phonon frequencies (around 1.2×10^{12} H_3) in which neither $\tau_{e\text{-ph}}^{-1}$ nor τ_{pt}^{-1} is effective. For $0.5\times10^8 < |X| < 1.5\times10^8$ dyn/cm^2, there are at least two large peaks in $\tau_{e\text{-ph}}^{-1}$ close to each other. As a result the whole region of low-frequency phonons is dominated by $\tau_{e\text{-ph}}^{-1}$ and relatively τ_b^{-1} becomes less important. It was also found that while the magnitudes of the higher-frequency peaks strongly depend upon E_u, the lower-frequency peaks remained nearly constant when E_u is changed. The behavior of the low-frequency peaks is consistent with the data of κ at high stress. Therefore at high values of stress ($> 1.5\times10^8$ dyn/cm^2), the high-frequency peaks which become smaller due to the increased Δ for the corresponding transitions are further shortened by a proper adjustment of the Bohr radii r_u. μ was estimated from the adjusted value of r_u at $X = -2.77\times10^8$ dyn/cm^2 and from this, r_u was calculated at $X = -1.0\times10^8$ dyn/cm^2. With this value of r_u and the values of A and L_c from Fig. 2, E_u was adjusted at $X = -1.0\times10^8$ dyn/cm^2 for the best fit of the phonon conductivity. η was found from E_u at $X = -1.0\times10^8$ dyn/cm^2 and E_{u0} and now the stage is set for the final calculation of phonon resistivity at all values of X.

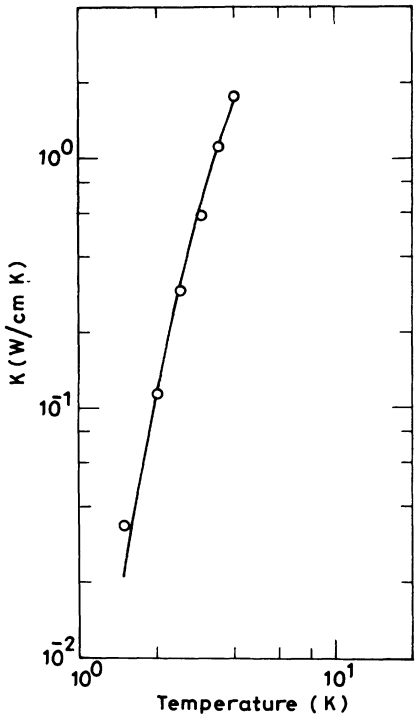

FIG. 3. Lattice thermal conductivity K at $X = 0$. Solid line shows the present calculations; circles are for the experimental results.

Figure 2 includes the improvised theoretical calculations as well as experimental results of thermal resistivity versus stress. Keyes and Sladek[1] also report the phonon-conductivity variation of a similar sample of Sb-doped Ge under constant stress -1.45×10^8 dyn/cm^2, but at 2.82 K the value of κ found from these data is higher ($=7.90\times10^{-1}$ W/cm K) than the one given in Fig. 2 ($=6.66\times10^{-1}$ W/cm K) at the same stress. This indicates an inaccuracy in the evaluation of stress. Keeping this inaccuracy in mind, the present theoretical explanation of κ versus stress at $T = 2.82$ K is quite satisfactory. Similarly, the same discrepancy among the theoretical and experimental values of phonon conductivity in Fig. 5 cannot be treated as the failure of the theory as suggested by earlier workers.[2,4] The appropriate theoretical description of the phonon conductivity around $T \approx 1$ K is still lacking even in the unstressed Sb-doped Ge and so a larger discrepancy at lower temperatures in Fig. 5 has not been taken care of.

As a matter of fact, E_u should also be level dependent. A decrease in the Bohr radius r of a particular level with stress will lower the value of E_u also. This would further increase the scope of modifying the theoretical results but due to the suspected inaccuracy in the experimental re-

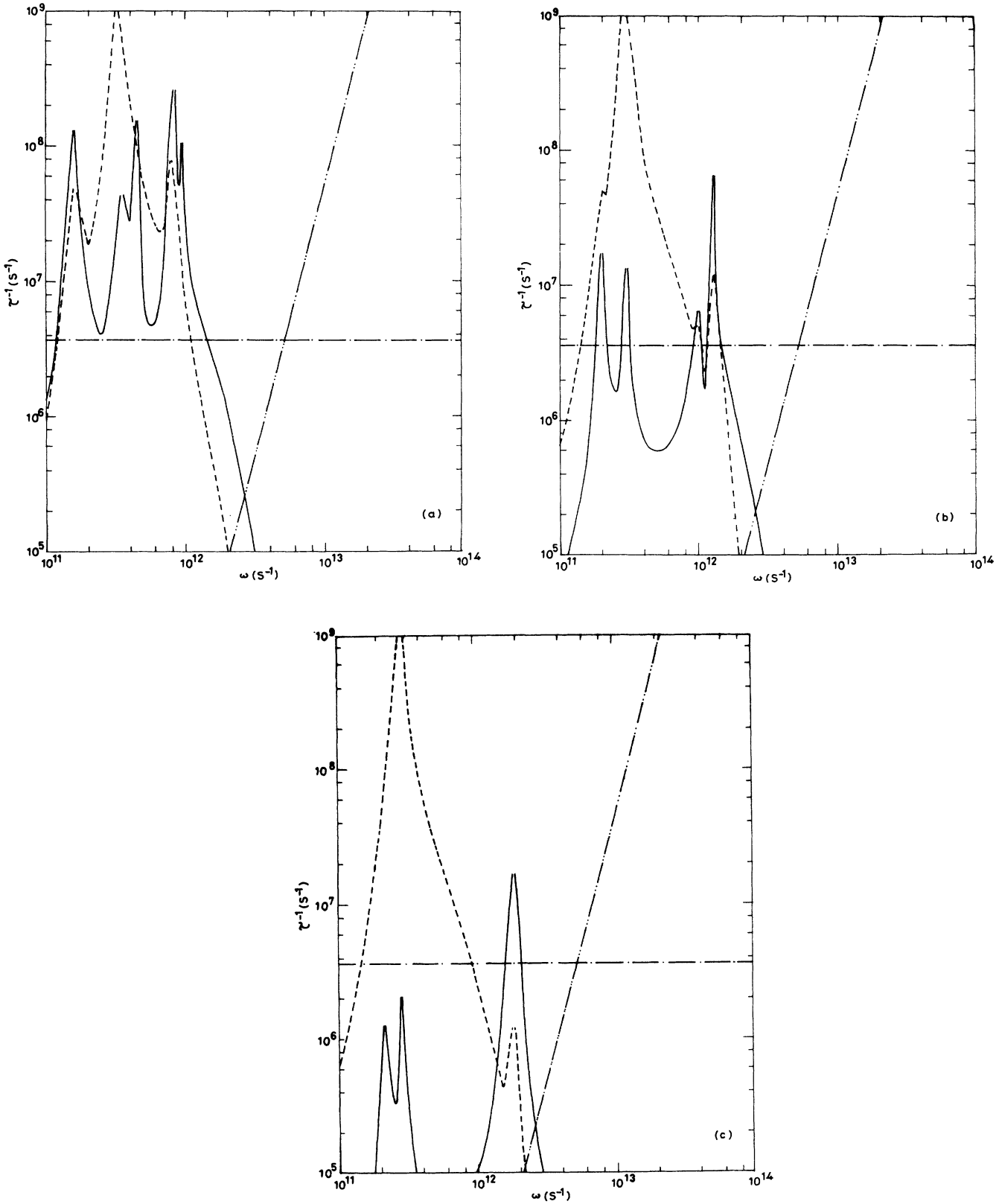

FIG. 4. Relaxation rates of the incoming longitudinal phonon as a function of angular frequency at $T=2.82$ K. Dashed line is for elastic and solid line represents absorption process (a) for $X=-0.50\times10^{8}$ dyn/cm^2, $E_u=16.225$ eV, $E_d=-8.0$ eV; (b) $X=-1.0\times10^{8}$ dyn/cm^2, $E_u=15.95$ eV, $E_d=-8$ eV; (c) $X=-1.50\times10^{8}$ dyn/cm^2, $E_u=15.6875$ eV, $E_d=-8$ eV; -.-.- for τ_b^{-1}; -..- for τ_{pt}^{-1}.

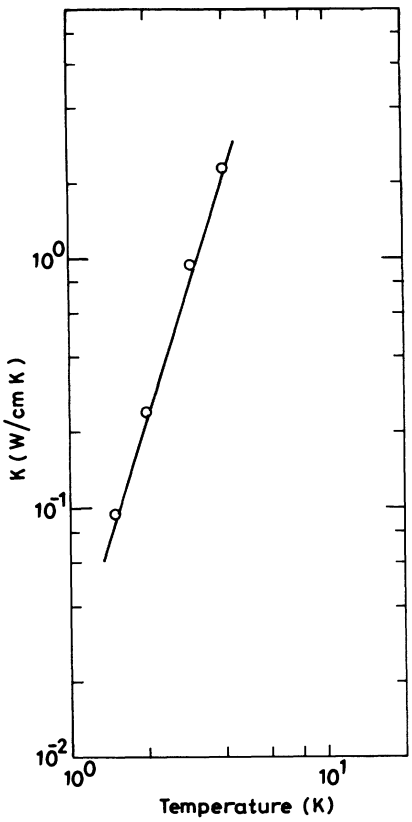

FIG. 5. Lattice thermal conductivity K at constant stress $X = -1.45 \times 10^8$ dyn/cm^2. Solid line represents the present calculations and circles are for the experimental data.

sults, we have not gone into this minor detail.

Lastly, the surface roughness as well as states would largely depend upon the stress. The thermal resistivity will definitely be better explained if stress smoothens the boundary, which, as reported earlier, becomes a strong source of phonon-scattering mechanism at high stress. This would also allow only a smaller rise of r with stress. This work, therefore, puts up a justification for the theory of electron-phonon scattering under stress. Unless sophisticated measurements of phonon conductivity, and the excitation spectra of doped semiconductors are done, failure of the theory for the [111] compression or tension should not be given importance. For example, the double degenerate level of the ground state corresponding to some donors in n-type Ge under [111] stress may split up due to internal random strains. Together with this the other effects, discussed in the paper, will probably lead to a correct analysis of the phonon-conductivity measurement under [111] uniaxial stress also.

ACKNOWLEDGMENTS

The authors wish to thank Professor G. S. Verma and Dr. V. J. Menon for some very useful discussions of this work. One of the authors (M.K.R.) would like to thank ICCR, Government of India for providing financial support to carry out this research.

*Permanent address: Department of Physics, University of Chittagong, Chittagong, Bangladesh.

[1]R. W. Keyes and R. J. Sladek, Phys. Rev. **125**, 478 (1962).
[2]A. Griffin and P. Carruthers, Phys. Rev. **131**, 1976 (1963).
[3]A. Griffin, J. Phys. Chem. Solids **26** 1909 (1965).
[4]K. Suzuki, Phys. Status Solidi B **78**, K77 (1976).
[5]K. Suzuki, Phys. Rev. B **11**, 3804 (1975).
[6]M. Singh and G. S. Verma, Phys. Rev. B **18**, 5625 (1978).
[7]S. Singh, Ph.D. thesis, Banaras Hindu University, 1979.
[8]W. Kohn and J. M. Luttinger, Phys. Rev. **98**, 915 (1955).
[9]H. Fritzsche, Phys. Rev. **125**, 1560 (1962).
[10]J. H. Reuszer and P. Fisher, Phys. Rev. **140**, A245 (1965); **165**, 909 (1968).
[11]M. Gorman and S. A. Solin, Phys. Rev. B **16**, 1631 (1977).
[12]M. K. Roy and K. C. Sood, Phys. Rev. B **44**, 11 085 (1991).
[13]W. Heitler, *Quantum Theory of Radiation,* 3rd ed. (Oxford University Press, London, 1954), Chap. 5.
[14]P. C. Kowk, Phys. Rev. **149**, 666 (1966).
[15]M. G. Holland, Phys. Rev. **132**, 2461 (1963).
[16]D. K. Wilson and G. Feher, Phys. Rev. **124**, 1068 (1961).
[17]P. J. Price, Phys. Rev. **104**, 1223 (1956).
[18]V. J. Tekippe, H. R. Chandrasekhar, P. F. Fisher, and A. K. Ramdas, Phys. Rev. B **6**, 2348 (1972).